50th AIAA Aerospace Sciences Meeting including the New Horizons Forum and Aerospace Exposition
09 - 12 January 2012, Nashville, Tennessee

AIAA 2012-0287

# Effect of plasma actuation on asymmetric vortex flow over a slender conical forebody

Xuanshi Meng[1], Jianlei Wang[2], Jinsheng Cai[3],
(*1. National Key Laboratory of Science and Technology on Aerodynamic Design and Research, Northwestern Polytechnical University, Xi'an 710072, China*)

Feng Liu[4], Shijun Luo[5]
(*2. The Department of Mechanical and Aerospace Engineering , University of California, CA 92697-3975, America*)



**The active flow control technology by using plasma actuation to manipulate forebody vortices on a slender conical body is being studied based on the previous research. This work is motivated by the need to increase the experimental velocity in the wind tunnel via an effective streamlining created by the actuators. A pair of Single-Dielectric Barrier Discharge (SDBD) plasma actuators is installed near the tip of a 20° circular-cone-cylinder model. The experiments are performed in a 3.0 m×1.6 m low speed wind tunnel at angles of attack of 45° and 50°. The test wind speed is varied from 15 m/s to 30 m/s with Reynolds numbers ranging from 0.16 to 0.32 million based on the cone base diameter. The results consist of measurements of circumferential pressure distributions over nine stations along the cone forebody, including one station using unsteady pressure tappings. The cross-sectional and overall side forces and yawing moments over the cone are calculated from the measured pressures. The experiments have confirmed that the plasma actuator can be used to achieve the proportional lateral control on slender forebodies at high angles of attack combined with a duty cycle technique. An effective control with a relative higher wind speed can be gotten by adjusting the position and induced flow direction of the plasma actuators.**

## Nomenclature

| | | |
|---|---|---|
| $C_n$ | = | yawing moment coefficient about cone base, yawing moment/$q_\infty SD$ |
| $C_p$ | = | pressure coefficient |
| $C_Y$ | = | overall side-force coefficient, overall side force/$q_\infty S$ |
| $C_{Yd}$ | = | time-averaged local side-force coefficient, local side force/$q_\infty d$ |
| $D$ | = | base diameter of circular cone forebody |
| $d$ | = | local diameter of circular cone forebody |
| $F$ | = | frequency of AC voltage source |
| $f^+$ | = | reduced frequency of actuator, $fD/U_\infty$ |
| $f$ | = | frequency of duty cycle |
| $L$ | = | length of circular cone forebody |
| $M$ | = | mach number |
| $q_\infty$ | = | free-stream dynamic pressure |
| $Re$ | = | free-stream Reynolds number based on D, $U_\infty D/v$ |
| $S$ | = | base area of circular cone forebody |
| $T$ | = | period of duty cycle |

[1] Post Doctor, Department of Fluid Mechanics.
[2] PHD Student, Department of Fluid Mechanics.
[3] Professor, Department of Fluid Mechanics.
[4] Professor, Department of Mechanical and Aerospace Engineering. Associate Fellow AIAA.
[5] Researcher, Department of Mechanical and Aerospace Engineering.

$t$ = time of duty cycle
$U_\infty$ = free-stream velocity
$V_{p\text{-}p}$ = amplitude of oscillation
$x, y, z$ = body coordinates, $x$ toward base, $y$ toward starboard, right-hand system
$\alpha$ = angle of attack
$\theta$ = meridian angle measured from windward generator, positive when clockwise
$\tau$ = fraction of time when starboard actuator is on over a duty-cycle period
$\nu$ = coefficient of kinematic viscosity

## I. Introduction

The demand for greater maneuverability requires fighter flight through large angles of attack. For many modern fighter aircraft, the nose portion of the fuselage consists of a long slender pointed forebody, over which the initially symmetric separation vortices become asymmetric as the angle of attack is increased beyond a certain value, causing large lateral aerodynamic loads[1-3]. In addition, conventional aerodynamic control surfaces become ineffective in such situations because of vortex wakes generated by the forebody.

Both computational and experimental research showed that the vortices are very sensitive to small perturbations near the apex of a forebody[4-6]. Although methods have been developed to delay the onset of asymmetric vortex shedding, the fact that the separation vortices generate large airloads and are very sensitive to small perturbations offers an exceptional opportunity for manipulating them with little energy input to achieve active lateral control of the vehicle in place of conventional control surfaces. Methods toward such a goal, by using various deployable mechanical devices and suction and blowing mechanisms, have been studied and reviewed by Malcolm[7] and Williams[8]. Most of these methods are based on steady methods in the sense that the control actuation is through a static or steady excitation.

The separation vortices exhibit a bistable mode of asymmetry, in which the vortices assume one of two mirror-imaged asymmetric configurations at high angles of attack[4,6,9]. Such bistable behavior makes continuous proportional control difficult to achieve with a conventional steady type of actuation. Bernhardt and Williams[10] used unsteady blowing near the forebody apex of an ogive-cylinder model and demonstrated the possibility of switching the flow from one of its asymmetric bistable modes to the other at 45° and 55° angle of attack. The proportional control has not achieved because the blowing was done either on the port or starboard side only.

Realizing that the flow may respond continuously to dynamic alternating excitations, Hanff et al.[11] alternated blowing from two forward facing nozzles near the apex of their test model to deliberately switch the vortices between their two bistable configurations with given duty cycles and at fast enough frequencies. Ming and Gu [12] used a miniature swinging strake mounted at the apex of their ogive cylinder model. They discovered that the flow would respond continuously to the mean angle settings if the frequency and amplitude of the oscillation of the strake are tuned appropriately. By using such ingenious unsteady dynamic controls, both groups succeeded in demonstrating the feasibility of proportional control on the side forces over slender ogive forebodies.

Plasma active flow control has received growing attention in recent years because of the advantages of not having mechanical parts, zero reaction time, broader frequency bandwidths and relatively low energy consumption. What is most important, the plasma actuators can be arranged conveniently on the parts surface of the vehicle. Many researchers choose the single dielectric barrier discharge (SDBD) as the plasma actuation type. The effect of the SDBD actuator is to impart momentum to the flow, much like flow suction or blowing but without the mass injection. Post and Corke[13,14] successfully demonstrated their use in the control of separation over stationary and oscillating airfoils. Huang et al.[15] also used them to control separation over turbine blades. A review is provided by Corke and Post[16]. Nelson et al.[17] used a pair of plasma actuators which located at the ±120° from the leeward meridian near the nose of a tangent ogive nose/cylindrical model to manipulate the forebody vortices. The experiments have confirmed that the plasma actuator can be used to displace the vortex on the forebody model by the Coanda effect.

Recently, Liu et al.[18] reported wind-tunnel experiments that demonstrate nearly linear proportional control of lateral forces and moments over a slender conical forebody at high angles of attack by employing a novel design of a pair of single dielectric barrier discharge (SDBD) plasma actuators near the cone apex combined with a duty cycle technique. Meng et al.[19] showed the linearity of the controlled lateral forces and moments with respect to the duty cycle can be improved via improved design parameters of the actuators.

The purpose of a great deal of research discussed above is to increase aircraft control capability at large angles of attack. For the practical super-maneuverability of a modern aircraft at high angles of attack, the flight speed is demanded beyond $0.1M$ at least. That is to say, if an active flow control technology can be incorporated on a

production aircraft, one of the essential condition is that it is effective at higher wind speed. But the active flow control technique on the slender forebody discussed above are almost performed at very low wind speeds and Reynolds number, especially for plasma flow control technique (as listed in table 1, some test speeds are calculated with Reynolds number and characteristic dimension, where ν is chosen as 14.9 million). The main objective of the following research is to increase the test velocity with effective plasma flow control via changing the position and the direction of the induced flow of the plasma actuator in comparison with the former research[18,19].

**Table 1. Brief Introductions of Some Forebody Vortex Control Experiments**

| Researchers | Experimental technique | Angles of attack | Reynolds number | Test speed (m/s) |
|---|---|---|---|---|
| John E. Bernhardt and David R. Williams[10] | Unsteady blowing | 45°, 55° | 6,300 | 3.3 (Calculated) |
| Ernest Hanff, Richard Lee and Richard J. Kind[11] | Unsteady blowing | 0°-70° | 176,000 | 40 (Presented) |
| Xiao Ming and Yunsong Gu[12] | Swinging strake | 55° | 20,000 | 4.8 (Calculated) |
| Takashi Matsuno, Hiromitsu Kawazoe and Robert C. Nelson[17] | Plasma actuation | 45° | 5,000 | 9.22 (Presented) |
| Feng Liu, Shijun Luo, Chao Gao, Xuanshi Meng et al.[18] | Plasma actuation | 30°-50° | 5,000 | 5.0 (Presented) |
| Tzong-Shyng Leu, Jeng-Ren Chang, Pong-Jeu Lu[21] | Flexible micro balloon actuators | 50°, 55° | 6,7000 | 20 (Presented) |

## II. Experimental Setup

### A. Wind-Tunnel Facility

The flow-control experiments are performed in a 3.0m×1.6m open-circuit low-speed wind tunnel at Northwestern Polytechnical University. The cone-cylinder model is tested at $\alpha = 45^\circ$ and $50^\circ$. The free stream velocity $U_\infty$ = 15 m/s～30m/s with Reynolds numbers ranging from 0.16 to 0.32 million based on the cone base diameter.

### B. Forebody Model configuration

Because the nose of any pointed forebody is locally conical in shape, the flow may be regarded as locally equivalent to that about a tangent cone. For this reason, an experimental model of a circular cone with a 10 deg semi-apex angle faired to a cylindrical afterbody is tested ( As that used in Ref. [18, 19]). The model consists of two separate pieces. The frontal portion of the cone is made of plastic and has a length of 150 mm. The rest of the model is made of metal. The total length of the cone is 463.8 mm with a base diameter of 163.6 mm.

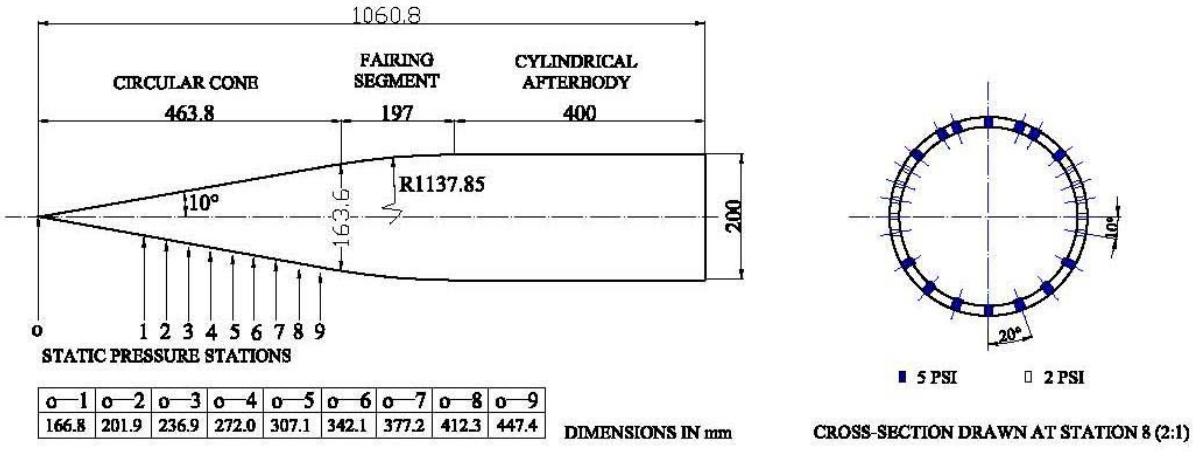


**Figure 1. The model and unsteady pressure tappings arrangements sketch**

The time-averaged pressure tappings are arranged in 10° increments around the azimuth of the cone at 8 stations (left in figure 1), so there are totally 36×8 pressures taps used to detect changes in the configuration of the vortices. The model of pressure taps is 9816 by the PSI Company with an accuracy of up to ±0.05% FS, which are read at frequency of 100 Hz. The sectional and overall side force, and yawing moment are calculated from the measured pressures. The sectional side-force coefficient $C_{Yd}$ is normalized with the local diameter d and is positive when pointing to the starboard side of the cone. The yawing moment coefficient $C_n$ is taken about the cone base and positive when yawing to the starboard side, and normalized with the base diameter $D$ and base area $S$. The model is carefully cleaned prior to each run of the wind tunnel.

### C. Design Concept of Single Dielectric Barrier Discharge Plasma Actuator

One pair of long strips of SDBD plasma-actuators are placed symmetrically on the plastic frontal cone near the apex as shown in Fig. 2(a). The plasma actuator consists of two asymmetric copper electrodes each of 0.03 mm thickness. A thin Kapton dielectric film wraps around the cone surface and separates the covered electrode from the exposed electrode as shown in Fig. 2(b). The length of the electrodes is 100 mm along the cone meridian with the leading edge located at 15 mm from the cone apex. The width of the exposed and covered electrode is 2 mm and 10 mm, respectively. There is no gap or overlap between the exposed and covered electrode.

The actuators are each connected to a high voltage ac source (model CTP-2000K by Nanjing Suman Co.) that provides about 13 kV peak-to-peak voltage sinusoidal excitation to the electrodes at a frequency of 8.5 kHz.

Three modes of operations of the actuators are defined. The plasma-off mode corresponds to the case when neither of the two actuators is activated. The plasma-on mode refers to the conditions when either the port or starboard actuator is activated while the other is kept off during the test. These are called the port-on and starboard on modes, respectively. The third mode employs a duty-cycle technique in which the two actuators on the cone is activated alternately with a specified duty cycle, $\tau$, defined as the fraction of time when the starboard actuator is on over a duty-cycle period. The fraction of time that the port actuator is on is then $1 - \tau$. The duty cycles are achieved by modulating the carrier AC voltage sources by a digital pulse wave generator. The optimum unsteady actuator frequency $f$ can be found such that $f^+ = 1$[20]. Comply with this rule, the duty-cycle frequency can be found at various free-stream velocity, which is 75 Hz, 150 Hz for 15 m/s, 30 m/s wind tunnel speed, respectively.

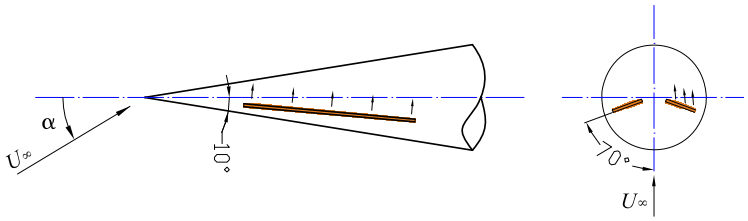


**a) α = 45°**

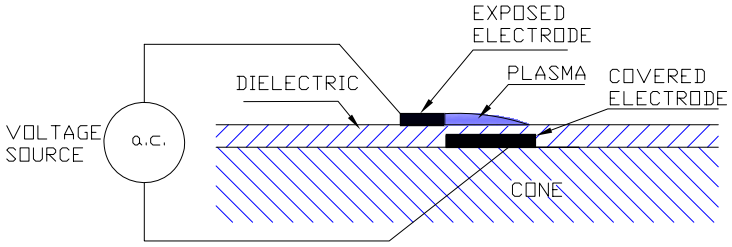


**b) Single Dielectric Barrier Discharge**

**Figure 2. Sketches of the plasma actuators.**

It should be pointed out that the design parameter is referred to the reference[17], but we make some changes. The right edge of the exposed electrode shown in Fig. 2 b) is aligned with the cone at the azimuth angle $\theta = \pm 70°$ ($\theta = \pm 60°$ in Reference[17]) which are nearer to the separation lines, where $\theta$ is measured from the windward meridian of the cone and positive is clockwise when looking upstream (Fig. 2 a)). The direction of the induced flow produced by actuators is downstream. The design idea for the position and the induced flow direction is intended to affect the boundary-layer separation positions via a plasma-induced Coanda effect. The actuators are hand-made and attached directly to the cone surface with no allowance.

## III. Experimental Results and discussion

### A. Base plasma-off flow

To check the flowfield states for plasma off, Figures 3 presents the time-averaged pressure distributions on odd-numbered measured stations at $\alpha = 45^\circ$ and $50^\circ$, $U_\infty = 15$ m/s. The sectional pressure distributions indicate the flow is essentially asymmetric around the cone.

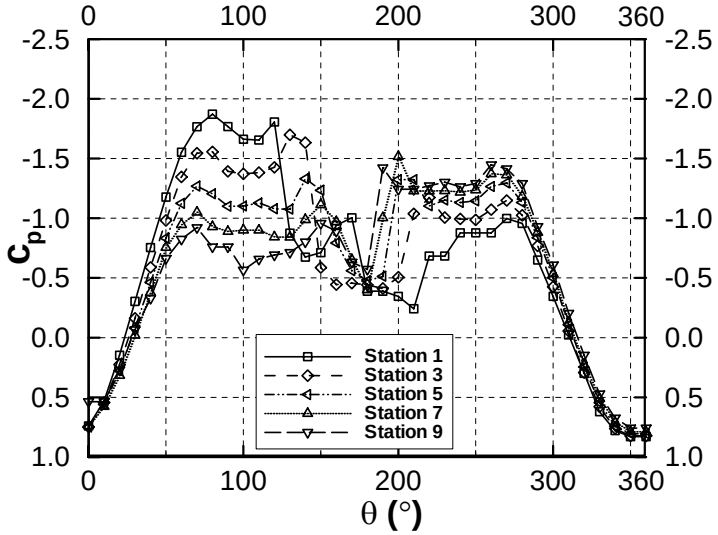


**a) $\alpha = 45^\circ$**

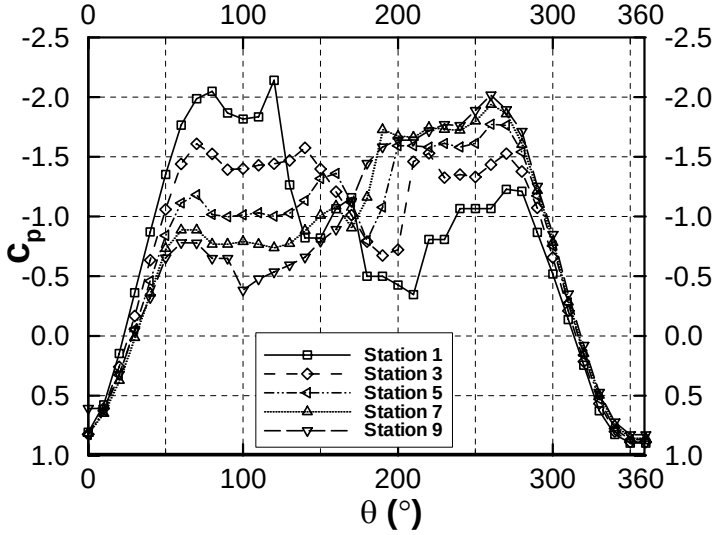


**b) $\alpha = 50^\circ$**

**Figure 3. Time-averaged pressure distributions over odd-numbered stations at $U_\infty = 15$ m/s, Plasma off.**

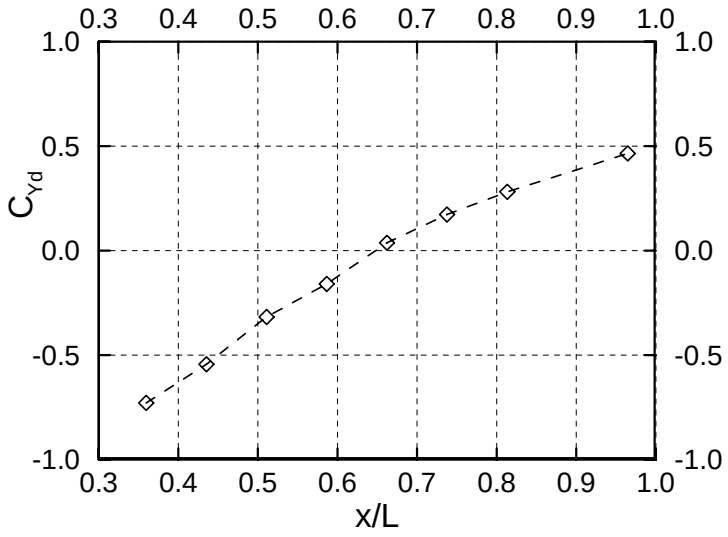


**a) $\alpha = 45°$**

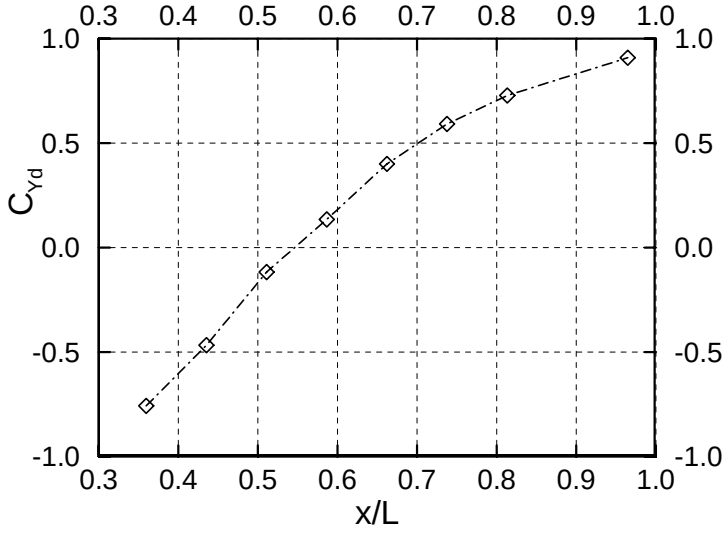


**b) $\alpha = 50°$**

**Figure 4. Time-averaged local-side force coefficient versus $x/L$ at $U_\infty = 15$ m/s, Plasma off.**

The local force distributions along the cone axis are calculated from the measured pressure data. Figure 4 present time-averaged local-side force $C_{Yd}$ versus $x/L$. It appears that $C_{Yd}$ would approach a non-zero limit when the variable $x$ approaches zero. Since $C_{Yd}$ is normalized by the local diameter $d$, the sectional side force is proportional to $d$ as the section approaches the body apex. Therefore, the pressure asymmetry does occur right at the apex of the body. This was observed in smoke visualization using a high-magnification lens by Zilliac et al. [4]. At $\alpha = 50°$, the $C_{Yd}$ is also changing with $x/L$, but the curve becomes much more nonlinear and the position where the signal from positive to negative is moved up from about $x/L = 0.65$ to $x/L = 0.55$.

As we see, the pressure distribution changes along the measured stations. Accordingly, $C_{Yd}$ is changing near linearly and from positive to negative, or vice versa between neighboring pressure stations. So we may refer that there are more than two vortices appearance along the cone segment. Tzong-Shyng Leu et al.[21] used the micro balloon actuators on a cone-cylinder slender body. The measurements results of X-type hot wire clearly indicate that a third vorticity-concentrated area is clearly found in the weak vortex side before and after the actuation. The appearance of the third vortices make the flowfeild over conical cone at $\alpha = 45°$ and 50° with 0.16 million Reynolds

number be not bistable. But it is seen from the pressure distributions that no vortex breakdown occurs over the cone forebody.

## B. Pressures, Lateral Forces and Moments with Plasma Control

Figure 5 presents the time averaged pressure distributions on odd-numbered Stations at $\alpha = 45^{\circ}$, $U_{\infty} = 15$ m/s for various cases, $\tau = 0.01-0.99$ denote plasma duty cycles. At measured station 1, when port plasma occupied the almost work time ($\tau = 0.01$), the higher suction peak appears on the port side of the cone, the pressure distributions are similar to that for plasma off. For various duty cycles ($\tau = 0.01-0.99$), the higher suction peak changes continuously from port side to starboard side. The pressure distributions for $\tau$, and $1 - \tau$ are not likely anti-symmetric, which may happen when the flowfeild is bistable. At measured station 3, the pressure distributions for $\tau$, and $1 - \tau$ are most likely symmetric, but not strictly. From station 5 to the rear measured stations, at $\tau = 0.01$, the higher suction peak appears on the starboard side of the cone, and it grows much higher continuously for various duty cycles.

Figure 6 present time-averaged local side force $C_{Yd}$ versus $\tau$ at $\alpha = 45^{\circ}$, it shows that proportional control of asymmetric force is achieved by the duty-cycled plasma actuations.

Figure 7 gives the overall side force coefficient $C_Y$ and yawing moment coefficient $C_n$ versus duty cycle $\alpha = 45^{\circ}$,. The linearity of the side force and yawing moment with respect to the duty cycle is improved over previous studies due to the improved design of the actuators.

Figure 8 presents the time averaged pressure distributions on odd-numbered Stations at $\alpha = 50^{\circ}$ , $U_{\infty} = 15$ m/s for various cases, At measured station 1, when $\tau = 0.01$, the higher suction peak appears on the port side of the cone, the pressure distributions is similar to that for plasma off. For various duty cycles ($\tau = 0.01-0.99$), the higher suction peak change continuously from port side to starboard side. The pressure distributions for $\tau$, and $1 - \tau$ are not likely anti-symmetric. At measured station 3, when $\tau = 0.01$, the pressure distribution is nearly symmetric. The suction peak occurs on starboard side and grows much higher continuously for various duty cycles. From station 5 to the rear measured stations, the higher suction peak appears on the starboard side of the cone, and it grows much higher continuously for various duty cycles. But the variation range is smaller than that at $\alpha = 45°$.

Figure 9 present time-averaged local side force $C_{Yd}$ versus $\tau$ at $\alpha = 50°$. it shows that proportional control of asymmetric force is achieved by the duty-cycled plasma actuations. Figure 10 gives the overall side force coefficient $C_Y$ and yawing moment coefficient $C_n$ versus duty cycle $\alpha = 50°$. The linearity of the side force and yawing moment with respect to the duty cycle is not so good as that at $\alpha = 45°$.

From time averaged pressure distributions changed with duty cycle ratios, we may find that the variation pattern of pressure distributions with plasma control under duty cycle model is determined at the measured station 1 which is closest to the plasma control region. For example, when $\alpha = 45°$, $U_{\infty} = 15$ m/s, the higher suction peak turns down at port side and the pressure magnitude of starboard side is increasing continuously for various duty cycles. This rule is worked for the rear measured stations no matter what the original (for plasma off) sectional pressure distribution is.

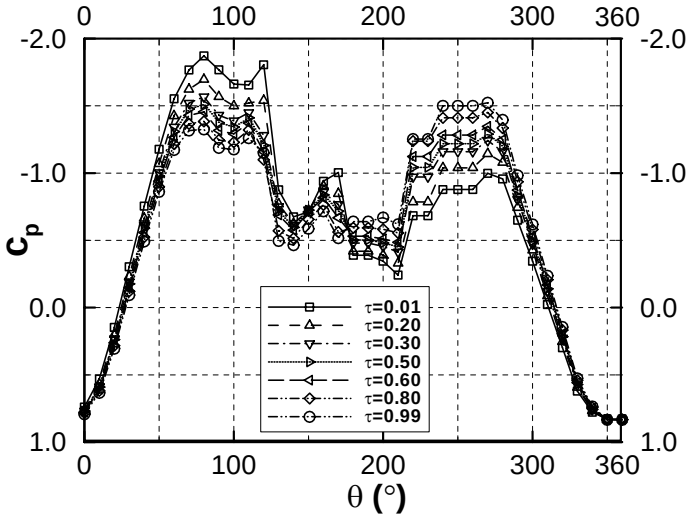


**a) Station 1**

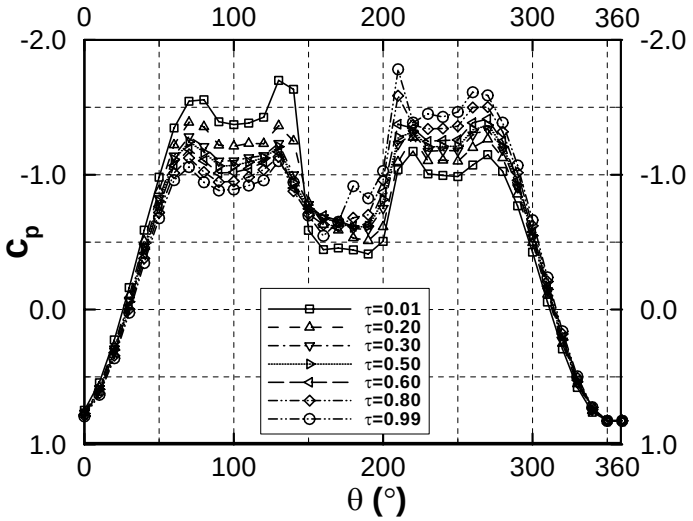


**b) Station 3**

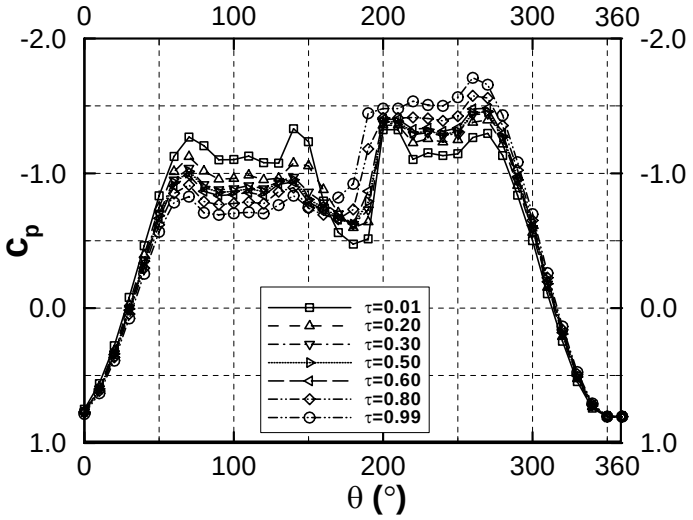


**c) Station 5**

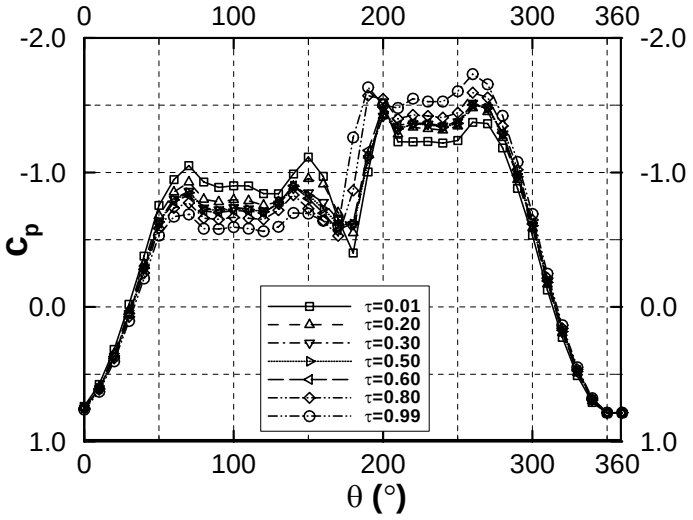


**d) Station 7**

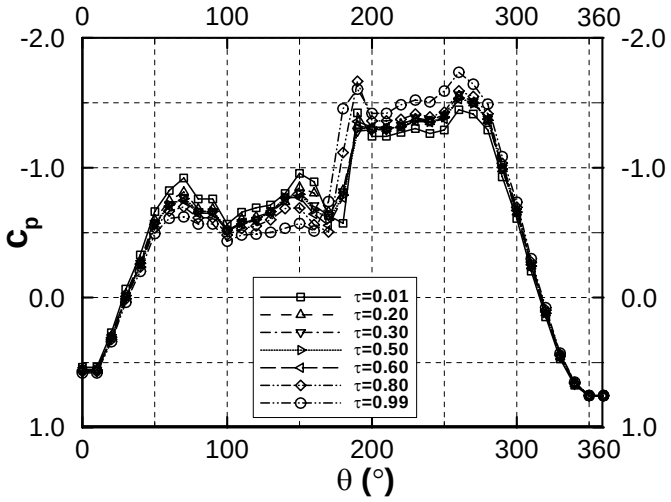


**e) Station 9**

**Figure 5. Comparison of time-averaged pressures for various duty cycles, odd Stations, $\alpha = 45°$ , $U_\infty = 15$**

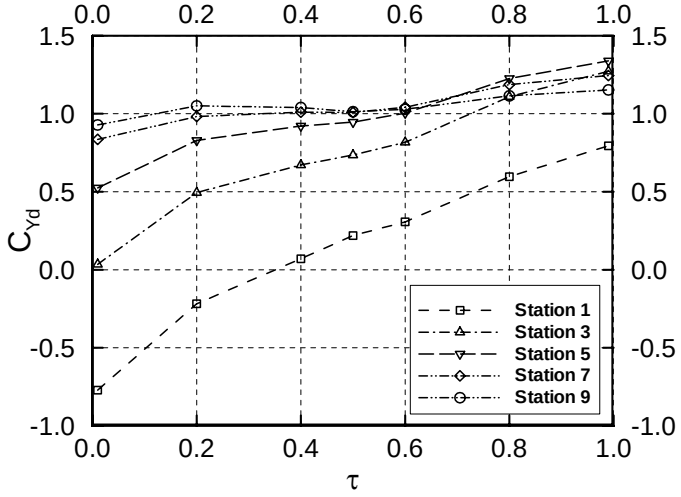


**Figure 6. Time-averaged local side force vs. duty cycle, $\alpha = 45°$ , $U_\infty = 15$ m/s.**

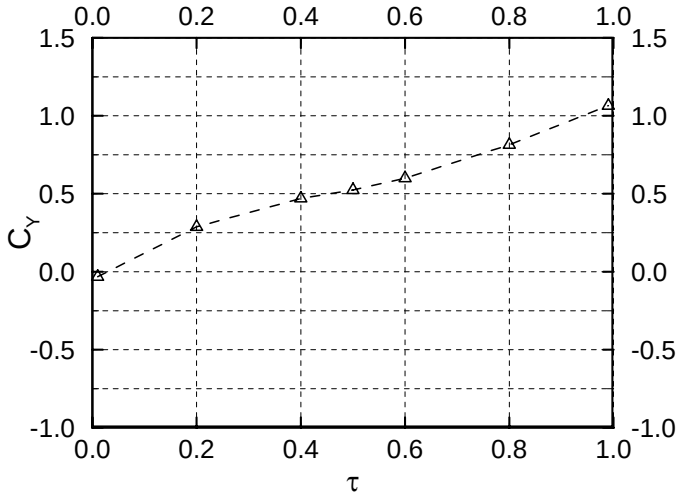


**a) Side force coefficient**

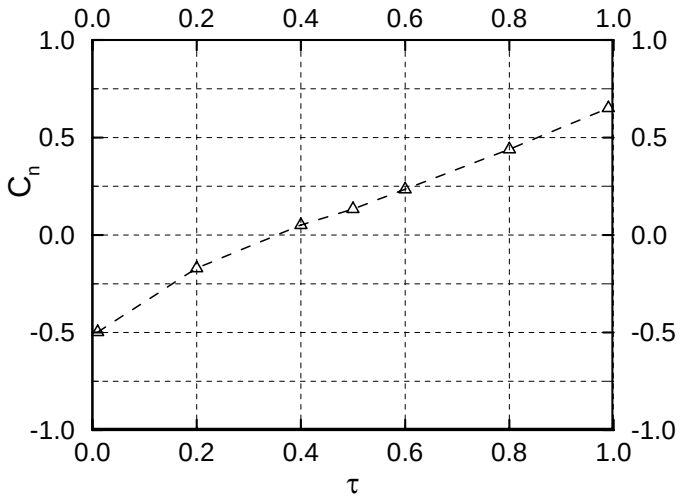


**b) yawing moment coefficient**

**Figure 7. Time-averaged overall side force and yawing moment vs. duty cycle, $\alpha$ = 45˚ , $U_\infty$ = 15 m/s.**

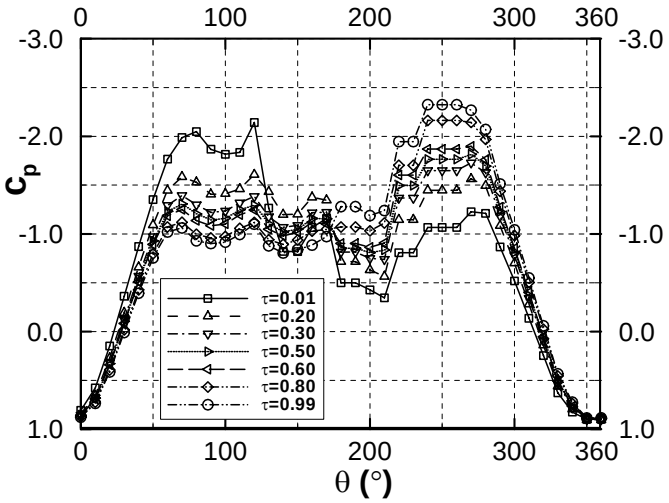


**a) Station 1**

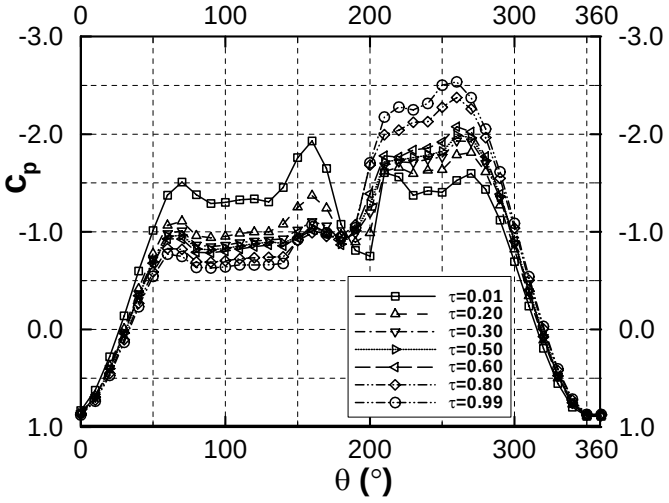


**b) Station 3**

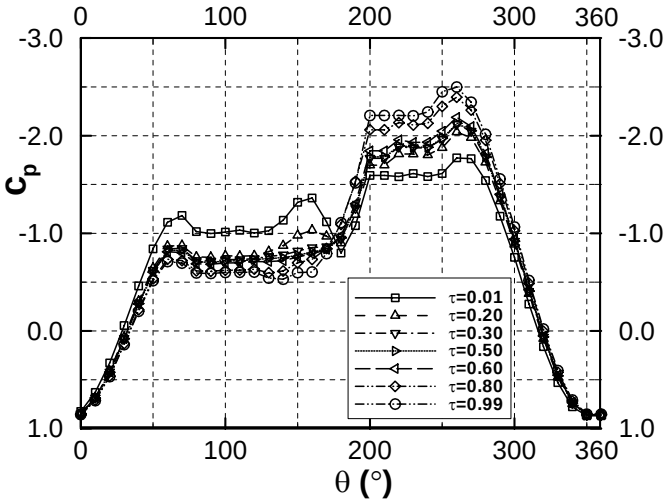


**c) Station 5**

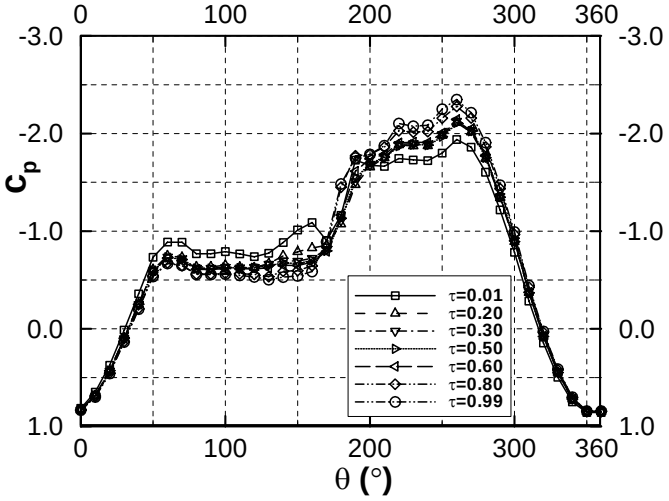


**d) Station 7**

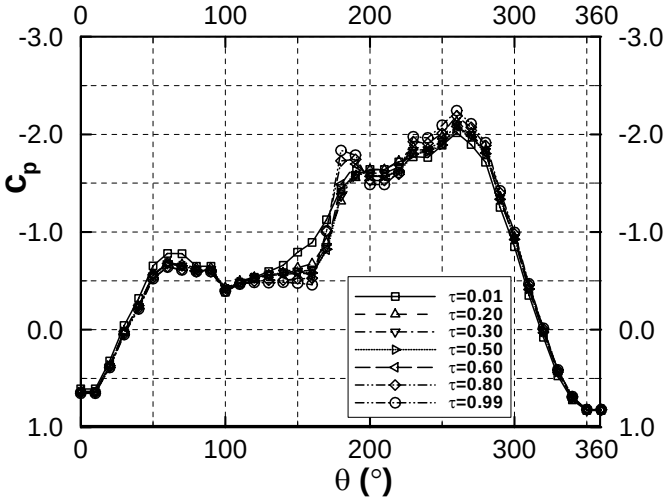


**e) Station 9**

**Figure 8. Comparison of time-averaged pressures for various duty cycles, odd Stations, $\alpha = 50^\circ$, $U_\infty = 15$ m/s.**

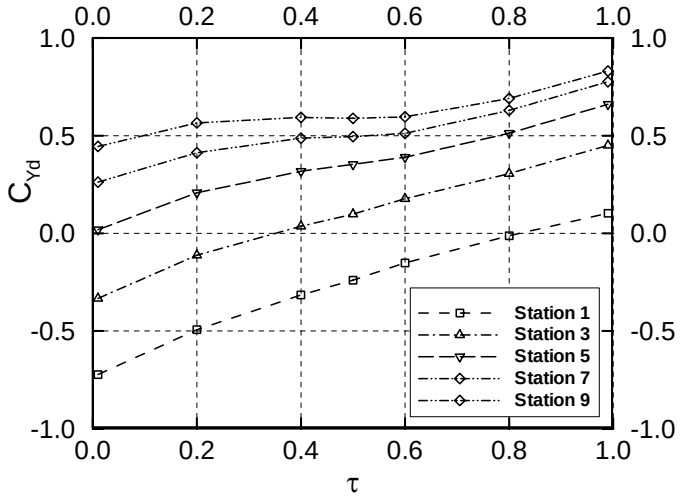


**Figure 9. time-averaged local side force vs. duty cycle, $\alpha = 50^\circ$, $U_\infty = 15$ m/s.**

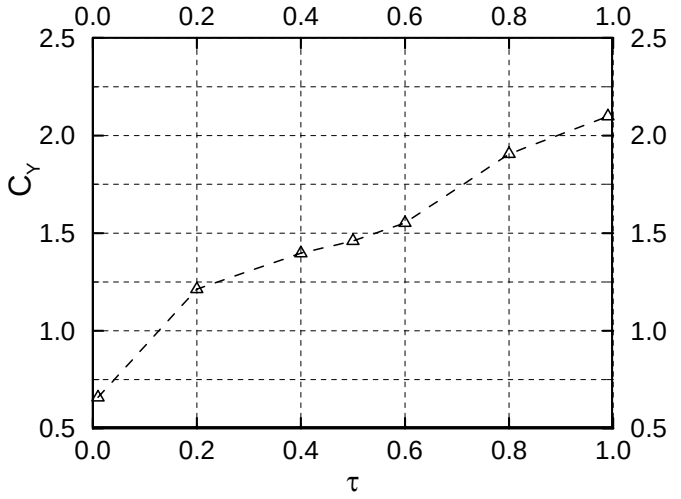


**a) Side force coefficient**

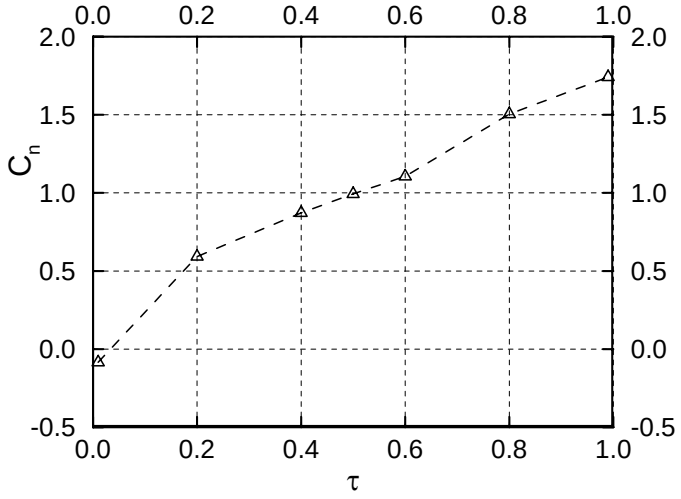


**b) yawing moment coefficient**

**Figure 10. Ensemble-averaged overall side force and yawing moment vs. duty cycle, $\alpha = 50^\circ$, $U_\infty = 15$ m/s.**

## C. Plasma Control with Higher Wind Speed

Experiments were performed for the plasma-off, starboard-on, and port-on modes at 30 m/s. The surface pressure distribution at station 1 with three control modes is shown in Figure 11 for $\alpha = 45^\circ$. The port-on results is almost overlap with those of the plasma-off result. Activating the starboard plasma actuator produces a clearly increase of the suction peak. The time-averaged local side force $C_{Yd}$ versus $x/L$ versus presents in figure 12 shown again that the variation pattern of pressure distributions with plasma control is determined at the plasma control region and then develops downstream.

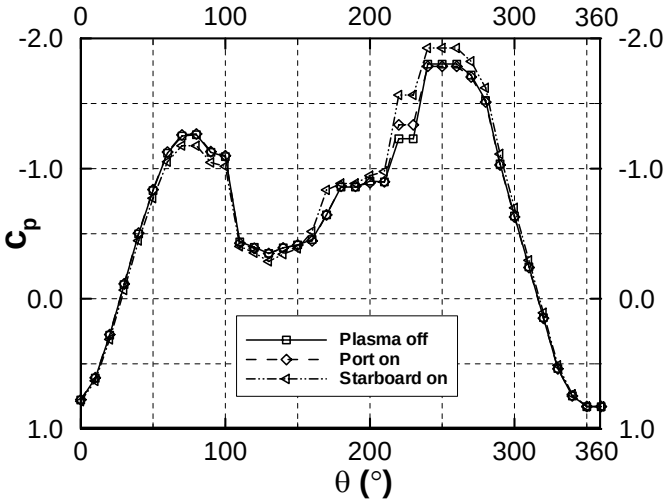


**Figure 11. Comparison of pressure distributions for the plasma-off and -on conditions at $\alpha = 45^\circ$, $U_\infty = 30$ m/s.**

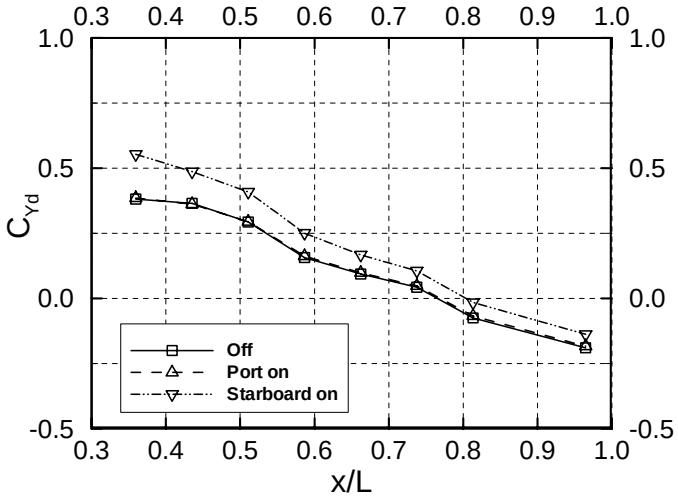


**Figure 12. Local side force distributions under plasma-off and -on conditions.**

## IV. Conclusions

An active flow control by using plasma actuation is performed in a low speed wind tunnel. The results of the present paper reconfirm previous findings that it is possible to achieve linear proportional control of the lateral forces and moments of a slender circular-cone body by the duty-cycled plasma flow control technique with appropriately designed plasma actuators and selected electric parameters. An effective control with a relative higher wind speed is gotten by adjusting the position and induced flow direction of the plasma actuators. The results is discussed through analyzing the pressure data obtained by time-averaged pressure tappings. By using the present actuator design parameters, the magnitude of port pressure turns down and that of the starboard side is increasing continuously for various duty cycle ratios no matter what the original (for plasma off) sectional pressure distribution

is. It shows that the variation pattern of pressure distributions with plasma control is determined at the plasma control region and then develops downstream.

## Acknowledgments

The present work is supported by *the National Natural Science Foundation of China* (51107101, 11172243) and *the Specialized Research Fund for the Doctoral Program of Higher Education* (200806990003, 20096102120001). The second author wishes to acknowledge support by *the Doctorate Innovation Foundation of Northwestern Polytechnical University through Grant CX201001* and *the Ministry of Education-funded PhD student academic Newcomer Award*. The authors would like to express their gratitude to Yongwei Gao, Zenghong Hui, Chunsheng Xiao, Lei Deng, Bin Tian, Shuai Zhao in Northwestern Polytechnical University for their valuable technical guidance and support in the wind-tunnel tests.

## References

[1]Allen H. J., Perkins E W., "Characteristics of flow over inclined bodies of revolution," 1951, NACA RM A50L07.
[2]Keener E. R, Taleghani J., "Wind Tunnel Investigations of the Aerodynamic Characteristics of Five Forebody Models at High Angles of Attack at Mach Numbers from 0.25 to 2. 1975", NASA TMX-73, 076.
[3]Ericsson L., "Sources of high alpha vortex asymmetry at zero sideslip," *Journal of Aircraft,* Vol. 29, No. 6, 1992, pp. 1086-1090.
[4]Zilliac G. G., Degani D., Tobak M., "Asymmetric vortices on a slender body of revolution," *AIAA J.*, Vol. 29, No. 5, 1991, pp. 667-675.
[5]Levy Y., Hesselink L., Degani D., "Systematic Study of the Correlation Between Geometrical Disturbances and Flow Asymmetries," *AIAA J.*, Vol. 34, No. 4, 1996, pp. 772–777.
[6]Cai J, Tsai H, Luo S, Liu F. Stability of Vortex Pairs over Slender Conical Bodies: Analysis and Numerical Computation. *AIAA J.*, Vol. 46, No. 3, 2008, pp: 712–722.
[7]Malcolm, G., "Forebody Vortex Control: A Progress Review," *AIAA Paper* 93-3540, Aug. 1993.
[8]Williams D., "A Review of Forebody Vortex Control Scenarios," *AIAA Paper* 97-1967, June 1997.
[9]Dexter, P., and Hunt, B. L., "The Effects of Roll Angle on the Flow over a Slender Body of Revolution at High Angles of Attack," *AIAA Paper* 81-0358, 1981.
[10]Bernhardt, J. E., and Williams, D. R., "Proportional Control of Asymmetric Forebody Vortices," *AIAA J.,* Vol. 36, No. 11, Nov. 1998, pp. 2087–2093.
[11]Hanff, E., Lee, R., and Kind, R. J., "Investigations on a Dynamic Forebody Flow Control System," Proceedings of the 18th International Congress on Instrumentation in Aerospace Simulation Facilities, *IEEE*, Piscataway, NJ, 1999, pp. 28/1–28/9.
[12]Ming, X., and Gu, Y., "An Innovative Control Technique for Slender Bodies at High Angle of Attack," *AIAA Paper* 2006-3688, June 2006.
[13]Post, M., and Corke, T. C., "Separation Control on High Angle of Attack Airfoil Using Plasma Actuators," *AIAA J.*, Vol. 42, No. 11, Nov. 2004, pp. 2177–2184.
[14]Post, M., and Corke, T. C., "Separation Control Using Plasma Actuators: Dynamic Stall Vortex Control on Oscillating Airfoil," *AIAA J.*, Vol. 44, No. 12, Dec. 2006, pp. 3125–3135.
[15]Huang, J., Corke, T. C., and Thomas, F. O., "Plasma Actuators for Separation Control of Low-Pressure Turbine Blades," *AIAA J.*, Vol. 44, No. 1, Jan. 2006, pp. 51–57.
[16]Corke, T. C., and Post, M., "Overview of Plasma Flow Control: Concepts, Optimization, and Applications," *AIAA Paper* 2005-563, Jan. 2005.
[17]Takashi Matsuno, Hiromitsu Kawazoe, Robert C. Nelson. "Aerodynamic Control of High Performance Aircraft Using Pulsed Plasma Actuators," *AIAA Paper* 2009-697, Jan. 2009.
[18]Liu F., Luo S. J., Gao C., Meng X. S., Hao J. N., Wang J. L., Zhao Z. J., "Flow Control over a Conical Forebody Using Duty-Cycled Plasma Actuators," *AIAA J.,* Vol. 46, No. 6, 2008, pp. 2969-2973.
[19]Meng Xuanshi, Guo Zhixi, Luo Shijun, Liu Feng, "Ensemble and Phase-Locked Averaged Loads Controlled by Plasma Duty Cycles," *AIAA Paper* 2010-878, Jan., 2010.
[20]Mehul Patel, Terry Ng, Srikanth Vasudevan, Thomas Corke, Martiqua Post Thomas McLaughlin, Charles Suchomel, "Scaling Effects of an Aerodynamic Plasma Actuator ," *AIAA Paper* 2007-635, Jan. 2007.
[21]Tzong-Shyng Leu, Jeng-Ren Chang, Pong-Jeu Lu, "Experimental investigation of side force control on cone-cylinder slender bodies with flexible micro balloon actuators," *Experimental Thermal and Fluid Science,* Vol. 29, 2005, pp. 909–918.